Three-dimensional Numerical Study of Natural Convection in a Cubical Enclosure with Two Heated Square Sections Submitted to Periodic Temperatures

Lahoucine Belarche [1], Btissam Abourida [2] and Touria Mediouni [3]

**[1] National School of Applied Sciences, Ibnou Zohr University
Agadir, Morocco**

**[2] National School of Applied Sciences, Ibnou Zohr University
Agadir, Morocco**

**[3] National School of Applied Sciences, Ibnou Zohr University
Agadir, Morocco**

Abstract

The three- dimensional numerical study of natural convection in a cubical enclosure, filled with air was carried out in this study. Two heating square sections are placed on the vertical wall of the enclosure. The imposed heating temperatures vary sinusoidally with time, in phase and in opposition of phase. The temperature of the opposite vertical wall is maintained at a cold uniform temperature and the other walls are adiabatic. The governing equations are solved using Control volume method by SIMPLEC algorithm. The sections dimension **D/L** and the Rayleigh number **Ra** were fixed respectively at 0,2 and 10^6. The temperature distribution, the flow pattern and the average heat transfer will be examined for a given set of the governing parameters, namely the amplitude of the variable temperatures $\boldsymbol{a}$ and their period $\boldsymbol{\tau_p}$. The obtained results show significant changes in terms of heat transfer and flow intensity, by proper choice of the heating mode and the governing parameters.

Keywords: *Three-dimensional modeling, Natural convection, Two square heated sections, variable heating, periodic temperature, dephasing.*

1. Introduction

The study of natural convection induced in cavities represents a great interest because of its direct application in various fields of engineering. Examples involving the natural convection phenomenon are building design, solar collectors, electronic and computer equipments and other applications which are referred to references [1-3]. In thermal control of electronic systems, a careful attention is necessary to ensure efficient design in order to optimize the cooling of the system. A review of the literature shows the existence of numerous numerical and analytical works on the subject. However, in most of these works, the studied configurations are two dimensional cavities, submitted to constant heating conditions. Hence, the two dimensional natural convection in a partially heated cavity (temperature or heat flux), with one or more heating portions, has been studied previously by many authors [4-8]. However, this state is not very representative of the reality happens in most practical applications. Indeed, in many situations, the energy supplied to the system varies over time giving rise to patterns of transient or unsteady natural convection. The solar energy collectors or electronic circuits are examples of such systems. The transient natural convection is then studied previously in the case of a cavity with time variable heating (temperature or heat flux) [9-15]. The previous results show that it is impossible to predict the fluid behavior and the heat transfer induced by variable heating conditions from the results obtained with constant thermal boundary conditions. In addition, it is noted that most of the published works adopted a two dimensional model. Few works have been reported on three-dimensional natural convection in enclosures partially heated [16-20], in spite of the fact that such approach reflects the phenomenon reality and leads to important and varied results, comparing to the two dimensional cases.

Note finally that all these available works on three-dimensional natural convection induced in a cavity partially heated, considered the case of constant heating temperature.

Hence, the purpose of the present investigation is to study numerically the case of laminar natural convection in a cubical enclosure with two heating square sections placed on its vertical wall. The imposed heating temperatures are varied sinusoidally with time, either in phase or in opposition of phase. The rest of the considered wall is adiabatic while the temperature of the opposite vertical wall is maintained at a cold uniform temperature and the other walls are adiabatic. The fluid flow motion, the temperature distribution and the average heat transfer will

be examined for a given set of the governing parameters, namely the amplitude of the variable temperatures *a* and their period τ_p.

2. Problem formulation

A schematic of the physical problem and coordinates are shown in figure 1. It consists of a cubical enclosure with two square sections placed on its left vertical wall. The rest of the wall is thermally insulated. The heating temperatures θ_{H1} and θ_{H2} of the sections are varied sinusoidally with time as shown in figure 2, in phase and in opposition of phase. The opposite vertical wall is maintained at uniform cold temperature θ_C, and the other walls are insulated.

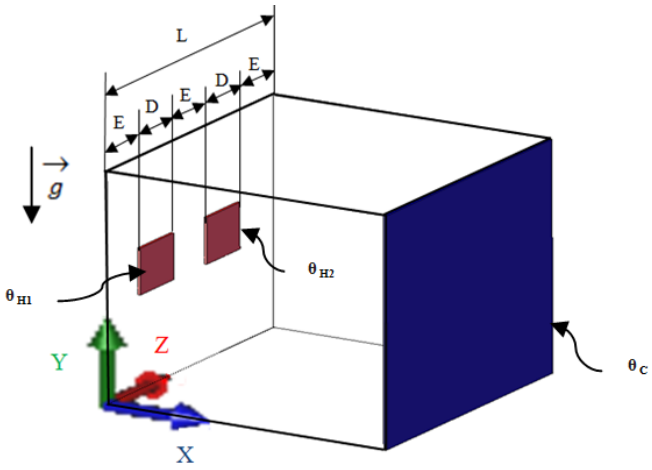

Fig. 1 Studied configuration and coordinates.

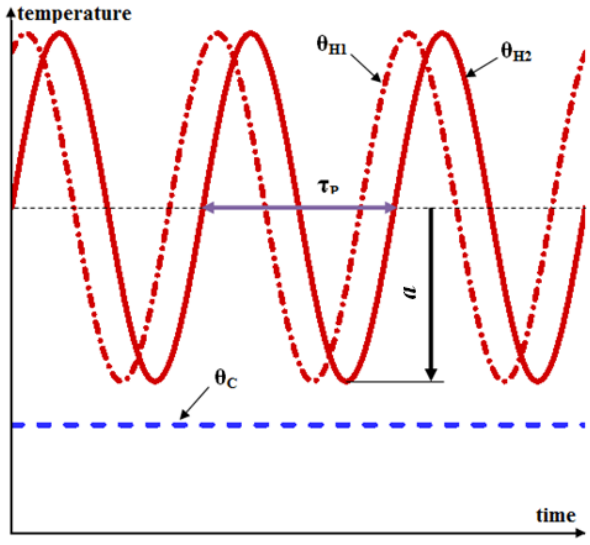

Fig. 2 Imposed thermal excitations.

The governing equations for laminar steady convection, using the Boussinesq approximation and neglecting the viscous dissipation, are expressed in the following dimensionless form

$$\frac{\partial U}{\partial X}+\frac{\partial V}{\partial Y}+\frac{\partial W}{\partial Z}=0 \quad (1)$$

$$\frac{\partial U}{\partial \tau}+\frac{\partial}{\partial X}(UU)+\frac{\partial}{\partial Y}(VU)+\frac{\partial}{\partial Z}(WU)=-\frac{\partial P}{\partial X}+\Pr\left(\frac{\partial^2 U}{\partial X^2}+\frac{\partial^2 U}{\partial Y^2}+\frac{\partial^2 U}{\partial Z^2}\right) \quad (2)$$

$$\frac{\partial V}{\partial \tau}+\frac{\partial}{\partial X}(UV)+\frac{\partial}{\partial Y}(VV)+\frac{\partial}{\partial Z}(WV)=-\frac{\partial P}{\partial X}+Ra\,\Pr\theta+\Pr\left(\frac{\partial^2 V}{\partial X^2}+\frac{\partial^2 V}{\partial Y^2}+\frac{\partial^2 V}{\partial Z^2}\right) \quad (3)$$

$$\frac{\partial W}{\partial \tau}+\frac{\partial}{\partial X}(UW)+\frac{\partial}{\partial Y}(VW)+\frac{\partial}{\partial Z}(WW)=-\frac{\partial P}{\partial X}+\Pr\left(\frac{\partial^2 W}{\partial X^2}+\frac{\partial^2 W}{\partial Y^2}+\frac{\partial^2 W}{\partial Z^2}\right) \quad (4)$$

$$\frac{\partial \theta}{\partial \tau}+\frac{\partial}{\partial X}(U\theta)+\frac{\partial}{\partial Y}(V\theta)+\frac{\partial}{\partial Z}(W\theta)=\left(\frac{\partial^2 \theta}{\partial X^2}+\frac{\partial^2 \theta}{\partial Y^2}+\frac{\partial^2 \theta}{\partial Z^2}\right) \quad (5)$$

The dimensionless variables used in these equations are defined as:

$$\left.\begin{aligned}&(X,Y,Z)=\left(\frac{x}{L},\frac{y}{L},\frac{z}{L}\right)\\&(U,V,W)=\left(\frac{uL}{\alpha},\frac{vL}{\alpha},\frac{wL}{\alpha}\right)\\&\tau=\frac{\alpha}{L^2}t\\&\theta=\frac{T-T_r}{\overline{T_H}-T_C}\quad\text{where}\quad T_r=\frac{\overline{T_H}+T_C}{2}\end{aligned}\right\} \quad (6)$$

In the above equations, the parameters Pr and Ra denote the Prandtl number, and the Rayleigh number, respectively. These parameters are defined as where

$$\Pr=\frac{\upsilon}{\alpha}\quad\text{and}\quad Ra=\frac{g\beta\,\Delta T L^3}{\alpha\upsilon} \quad (7)$$

The hydrodynamic boundary conditions are such as the velocity components are zero on the rigid walls of the enclosure (U = V = W = 0). The dimensionless thermal boundary conditions associated to the governing equations are:

- Heating section 1 :

$$\theta_{H1}=0.5+a\sin\left(\frac{2\pi\tau}{\tau_p}\right)\ \text{at}\ \frac{(1-2D/L)}{3}<Z<\frac{(1+D/L)}{3},\quad \frac{(1-D/L)}{2}<Y<\frac{(1+D/L)}{2}\ \text{and}\ X=0 \quad (8a)$$

- Heating section 2 :

$$\theta_{H2}=0.5+a\sin\left(\frac{2\pi\tau}{\tau_p}+\varphi_P\right)\ \text{at}\ \frac{(2-D/L)}{3}<Z<\frac{(2+2D/L)}{3},\quad \frac{(1-D/L)}{2}<Y<\frac{(1+D/L)}{2}\ \text{and}\ X=0 \quad (8b)$$

- Elsewhere on the left vertical wall:

$$\frac{\partial \theta}{\partial n} = 0 \tag{8c}$$

- Right vertical wall:

$$\theta_C = -0.5 \text{ at } X = 1 \tag{8d}$$

- Other vertical and horizontal walls

$$\frac{\partial \theta}{\partial n} = 0 \tag{8e}$$

Where n is the normal direction to the considered wall and a, τ_p and φ_P are respectively the amplitude of the heating temperature, its period and the dephasing between the two heating temperatures. The amplitude a and the period τ_p is defined respectively, as:

$$\tau_P = \frac{\alpha}{L^2} t_P \text{ and } a = \frac{A}{\overline{T_H} - T_C} \tag{9}$$

The average heat flux on the cold wall is calculated at each time step by:

$$Nu = \left(\int_0^1 \int_0^1 \left. \frac{\partial \theta}{\partial X} \right|_{x=1} dYdZ \right) \tag{10}$$

The mean Nusselt number characterizing the heat transfer through the right wall is evaluated as:

$$\overline{Nu_C} = \frac{1}{\tau_{Nu}} \int_0^{\tau_{Nu}} \left(\int_0^1 \int_0^1 \left. \frac{\partial \theta}{\partial X} \right|_{x=1} dYdZ \right) d\tau \tag{11}$$

τ_{Nu} represent the period of Nusselt temporal variations.

3. Numerical method

The Navier-Stokes and energy equations are discretized by the finite volume method developed by Patankar [21] adopting the power law scheme. To overcome the difficulty associated with the determination of the pressure, we suggest solving the equations of conservation of momentum coupled with the continuity equation using the SIMPLEC algorithm. For solving the algebraic system obtained after discretization of partial differential equations, the Alternating Direction Implicit scheme (ADI) is used. Tridiagonal system obtained in each direction is solved using the THOMAS algorithm. Convergence of the numerical code is established at each time step according to the following criterion, which fixes the relative difference between the field variables ϕ (= U, V, W,T,P), in successive time steps (n and n+1) less than 10^{-5}.

$$\sum_{i,j,k=1}^{i\max, j\max, k\max} \frac{\left| \phi_{i,j,k}^{n+1} - \phi_{i,j,k}^{n} \right|}{\left| \phi_{i,j,k}^{n} \right|} \leq 10^{-5} \tag{12}$$

i, j and k are the grid positions.

The flow pattern obtained in the case of constant heating was used as the as initial condition for the numerical calculations conducted in the case of variable heating temperature in order to favour the convergence of the numerical code.

To check the effect of grid size, preliminary tests were conducted for different combinations of the governing parameters. Table 1 shows the values of time averaged Nusselt number, Nu_c obtained for different grid sizes in the case D/L = 0.2, $\tau_p = 0.8$, $a = 0.8$ and Ra = 10^6.

To obtain a fine mesh at the active walls (X = 0 and X = 1), the computational domain was discretized by adopting a non-uniform mesh in the X direction and uniform in directions Y and Z.

The grid size effect on Nusselt number calculated using Eq.10 is presented in table 1 in the case of constant heating temperatures. The results induced by the grid 41×41×41 differs by less than 2% from those obtained with a refined grid 71×71×71. Hence, the non uniform staggered grid of 41×41×41 nodes was estimated to be appropriate for the present study since it permits a good compromise between the computational cost (a significant reduction of the execution time) and the accuracy of the obtained results.

Finally, the accuracy of the developed numerical code was checked by comparing the present results, obtained for constant heating temperature with those previously published by Fusegi et al. [22] in the case of cubical enclosure with a completely heated vertical wall and by Frederick et al. [19] in the case of cubical enclosure with a partially heated wall (s/L = 0.3). A comparison of the averaged Nusselt number Nu, and maximum values velocities U and V, in the mid-plane Z = 0.5 is given in Table 2 for Ra = 10^6. The obtained results show excellent agreement with the two references, with maximum differences not exceeding 3.38% for Nu, 2.45% and 3.87% respectively for U_{max} and V_{max} comparing to Fuseigi's results [22] and 2.38% for Nu, 2.045% and 3, 34% respectively for U_{max} and V_{max} comparing to Frederik result's [19].

Table 1: Effect of the grid size on Nu_c for D/L = 0.2, $\tau_p = 0.8$, $a = 0.8$ and Ra =10^6

Maillage	$\overline{Nu_C}$
31x31x31	2.06668
41x41x41	2.17545
51x51x51	2.19938
61x61x61	2.20852
71x71x71	2.21896

Table 2: Validation of the numerical code against published results in terms of Nu, U_{max} and V_{max} for Ra =10^6

	Nu	**U_{max}**	**V_{max}**
Fusegi et al. [22]	8.77	0.08416	0.2922
Present work	9.066	0.08622	0.3035
Difference (%)	3.38	2.45	3.87
Frederic et al. [19]	3.4857	58.3830	151.693
Present work	3.5687	58.5024	152.1997
Difference (%)	2.38	2.045	3, 34

4. Results and discussion

In this section, we present the effects of the period, amplitude and heating mode on temporal evolutions of maximum velocity in the mid-plane of the cavity (U_{max}) and the heat loss through its cold wall (Nu_c). The average values are compared for different sets of the amplitude and the period. We also present streamlines and isotherms produced during a flow cycle for each type of heating mode in order to illustrate the behavior of the fluid motion and the heat exchange in the cavity due to the thermal excitation. Due to the big number of governing parameters, we choose to fix the Rayleigh number Ra and the heating sections dimension to respective values of 10^6 and 0.2. This choice, which characterizes adequately the fluid motion and heat transfer phenomenon in the cavity, was made after many numerical simulations conducted for different Ra and different D/L. Hence, the results presented in this paper are obtained for fixed Ra = 10^6, D/L = 0.2 and Pr = 0.71 (air) and varied $0 \le a \le 1$, $0 \le \boldsymbol{\tau_P} \le 1$ and $\rho = 0$ or π.

4.1 Influence of the period

To illustrate the effect of the parameter $\boldsymbol{\tau_P}$, we present the temporal evolution of U_{max} (calculated in the plane Z = 0.5) and Nu_c for different modes of heating, a = 0.8 and Ra = 10^6. Thus, figures 3a and 3b show respectively the temporal evolutions of U_{max} and Nu_c obtained in the case of the two imposed temperatures (θ_{H1} and θ_{H2}) varying in phase for $0.1 \le \tau_P \le 0.4$. These figures show that all the obtained solutions are periodic, with resulting periods equal to those imposed on the exciting temperatures. We also note that the sinusoidal nature of oscillations is maintained in the Nu_c evolution, but disappears in the case of U_{max} when the period increases. The observed rate is due to the fact that the imposed temperatures have low values in a part of the cycle and gives rise to a special fluid motion as seen in the streamlines presentation (figures 6a-6b and 6g-6h). In addition, the oscillation amplitudes of U_{max} undergo significant decreases when τ_P is increased, while those of Nu_c increased with τ_P. For the same conditions as before, we examine the effect of the period in the case of two imposed temperatures (θ_{H1} and θ_{H2}) varying in opposite of phase. Thus, Figures 4a and 4b show respectively the temporal evolutions of U_{max} and Nu_c obtained in the case of the two imposed temperatures (θ_{H1} and θ_{H2}) varying in opposition of phase for $0.1 \le \tau_P \le 0.4$. These figures show that the obtained solutions are also periodic. But, the resulting periods are equal to half of those imposed on the exciting temperatures. We also note the sinusoidal nature of oscillations is conserved in the evolution of Nu_c, but not for U_{max}. The maximum amplitudes of oscillation of U_{max} undergo significant decreases when τ_P is increased, while those of Nu_c increase with τ_P. These trends are similar to those encountered in the case of the two imposed temperatures varying in phase (figures 3a and 3b). However, compared to the constant heating values (dashed lines), the resulting Nuc values seems to be greater all the time, in the case of opposition of phase variation. In addition, the velocity U_{max} shows a double periodicity which is not observed in the previous case (phase variation) and can denote a special flow motion inside cavity as it can be seen in the following paragraph.

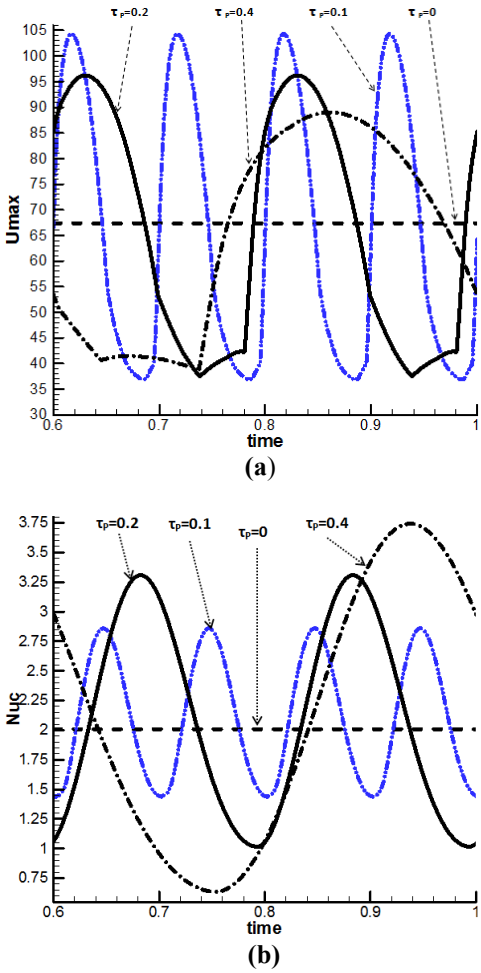

Fig. 3 Effect of $\boldsymbol{\tau_P}$ for a = 0.8 and Ra = 10^6 in the case of two temperatures varying in phase: a) U_{max} and b) Nu_c.

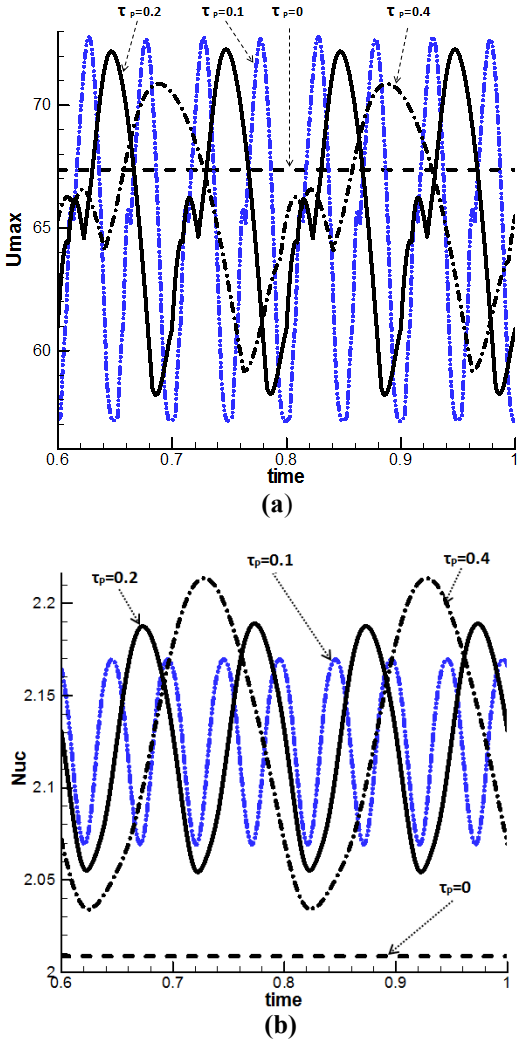

Fig. 4 Effect of τ_P for a = 0.8 and Ra = 10^6 in the case of two temperatures varying in opposition of phase: a)U_{max} and b)Nuc

4.2 Isotherms and streamlines

In order to study the details of the flow and heat transfer within the cavity, isotherms and flow lines are produced for each heating mode, during a flow cycle for Ra = 10^6, D/L = 0.2, a = 0.8 and τ_P = 0.2. The corresponding instants are chosen during a flow cycle of velocity U_{max} (figures 5a and 5b). The heating temperatures evolution is also presented in these figures to illustrate their direct effect on the flow structure and the heat exchange.

Hence, figures 6a to 6h show isotherms (on the left) and streamlines (on the right), corresponding to the instants (a) to (h) in Figure 5a when the two imposed temperatures are varying in phase. For more visibility of the fluid motion, streamlines are presented at the mid-plane of the cavity (X = 0.5). Further flow presentations were produced for different plans in the cavity, and show that the flow consists of a single cell, turning clockwise and presenting a symmetry relative to the center of the cavity (Z = 0.5) all the time. The cell intensity varies during the cycle.

Initially, when the imposed temperatures take their lowest values, the streamlines are straight and vertical while the heat exchange is very weak through the cavity (Figure 6a). Evolving in time, two small cells-rotating in opposite directions-appear on the upper corner of the cavity (Figure 6b). The intensity of these cells increases (figure 6c) and reaches a maximum value as it is seen in figure 6d. This instant correspond to a maximum heating period as shown in figure 5a. After that, a heating temperatures decrease leads to a flow intensity and heat exchange diminution (Figures 6f to 6h). Generally, we can note that the isotherms and the streamlines present a symmetry relative to the plan Z=0.5 during the entire cycle flow, when the two heating temperatures are varied in phase.

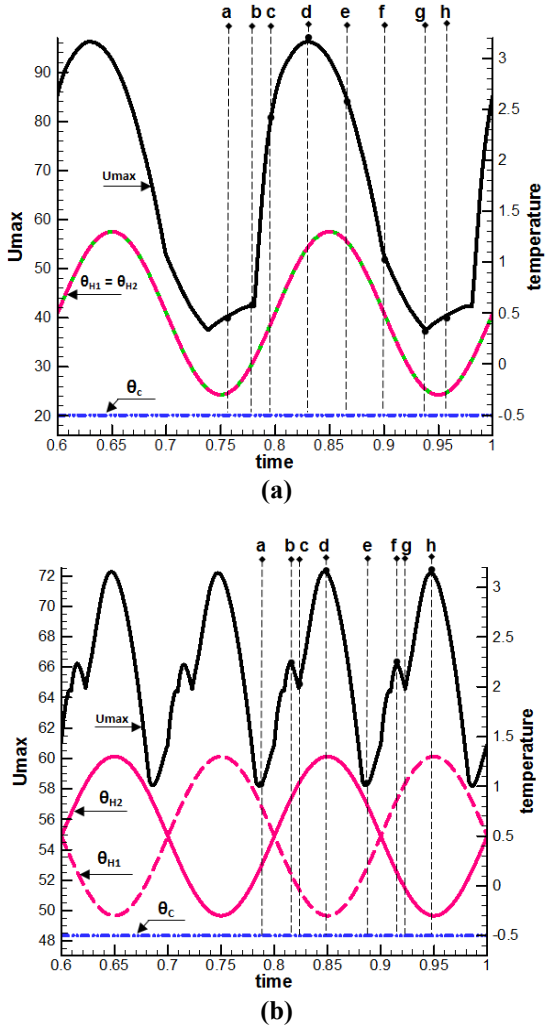

Fig. 5 Temporal variations of U_{max} for τ_P = 0.2 and a = 0.8, and excitation temperatures: a) in phase, b) in opposition of phase.

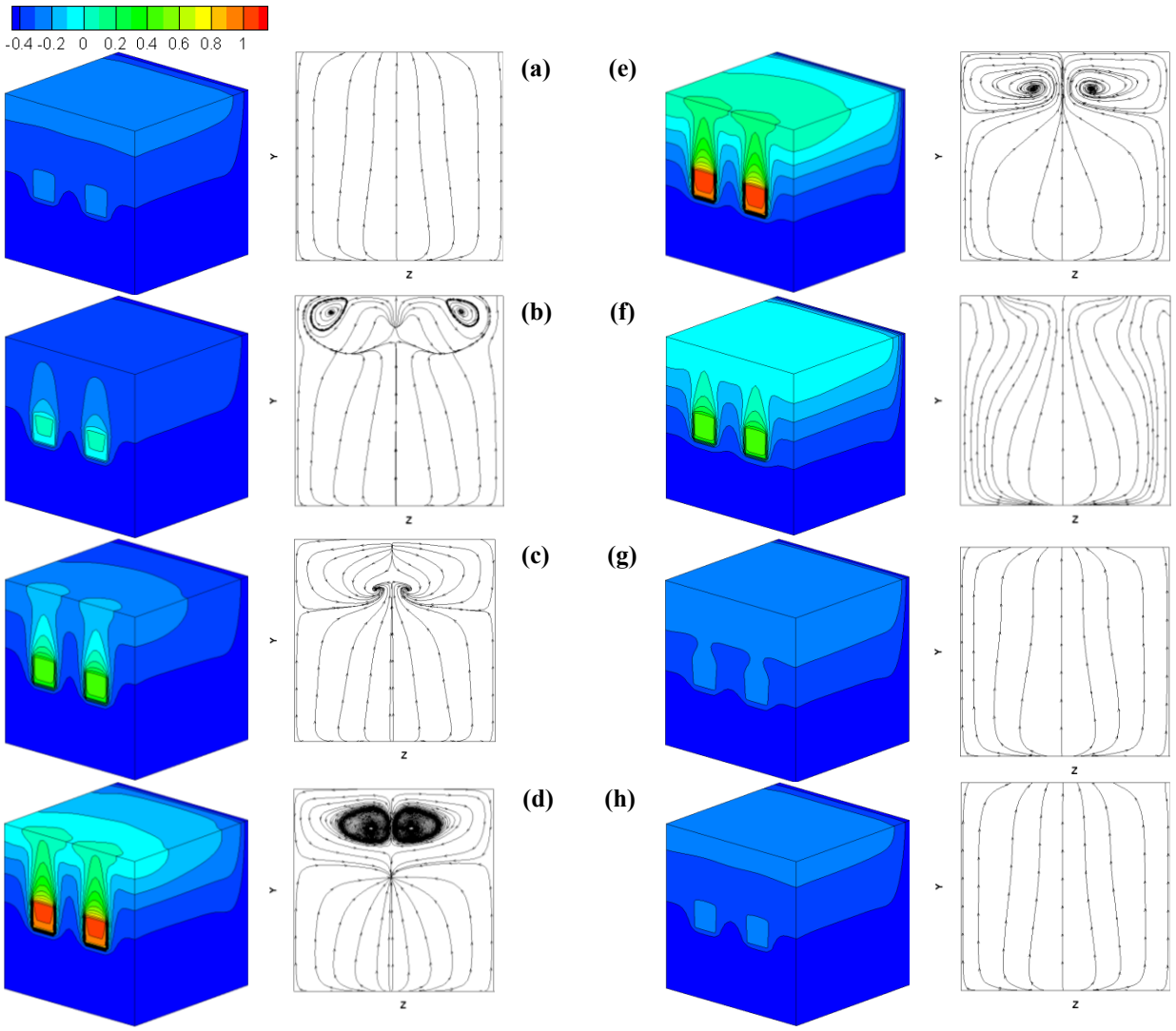

Fig. 6 Isotherms and streamlines (at plan X = 0.5) over one cycle for Ra = 10^6, a = 0.8 and τ_P = 0.2 in the case of two temperatures varying in phase.

Figures 7a-7h show the dynamic and thermal behaviors obtained when the two imposed temperatures are varied in opposition of phase. The corresponding instants are checked out in figure 5b. It can be seen from this figure that a single heating period leads to a double resulting period of U_{max}. This behavior wasn't encountered in the case of two heating temperatures varying in phase and can explain the absence of symmetry relative to the center of the cavity (Z = 0.5), observed in the previous case.

Hence, the heating section becomes in turn the major source of heating and leads to recirculation cells in the top of the cavity. These cells are placed in the opposite upper corner of the cavity, according to the dominant heater section position (figures 7a-7h).

4.3 Mean values

In order to study the effect of the heating mode on mean heat transfer, figures 8a and 8b illustrate the average values of $\overline{Nu_C}$ versus the period τ_P for different amplitudes a, when the imposed temperatures are respectively varied in phase and in opposite of phase. The value corresponding to the case of constant heating source temperature (a = 0) are also presented in the same figures as references. It should be noted that for all the considered values of a, the presented function remain close to the permanent value in the case of weak periods. This indicates an insensitivity of the system with respect to the imposed thermal excitation.

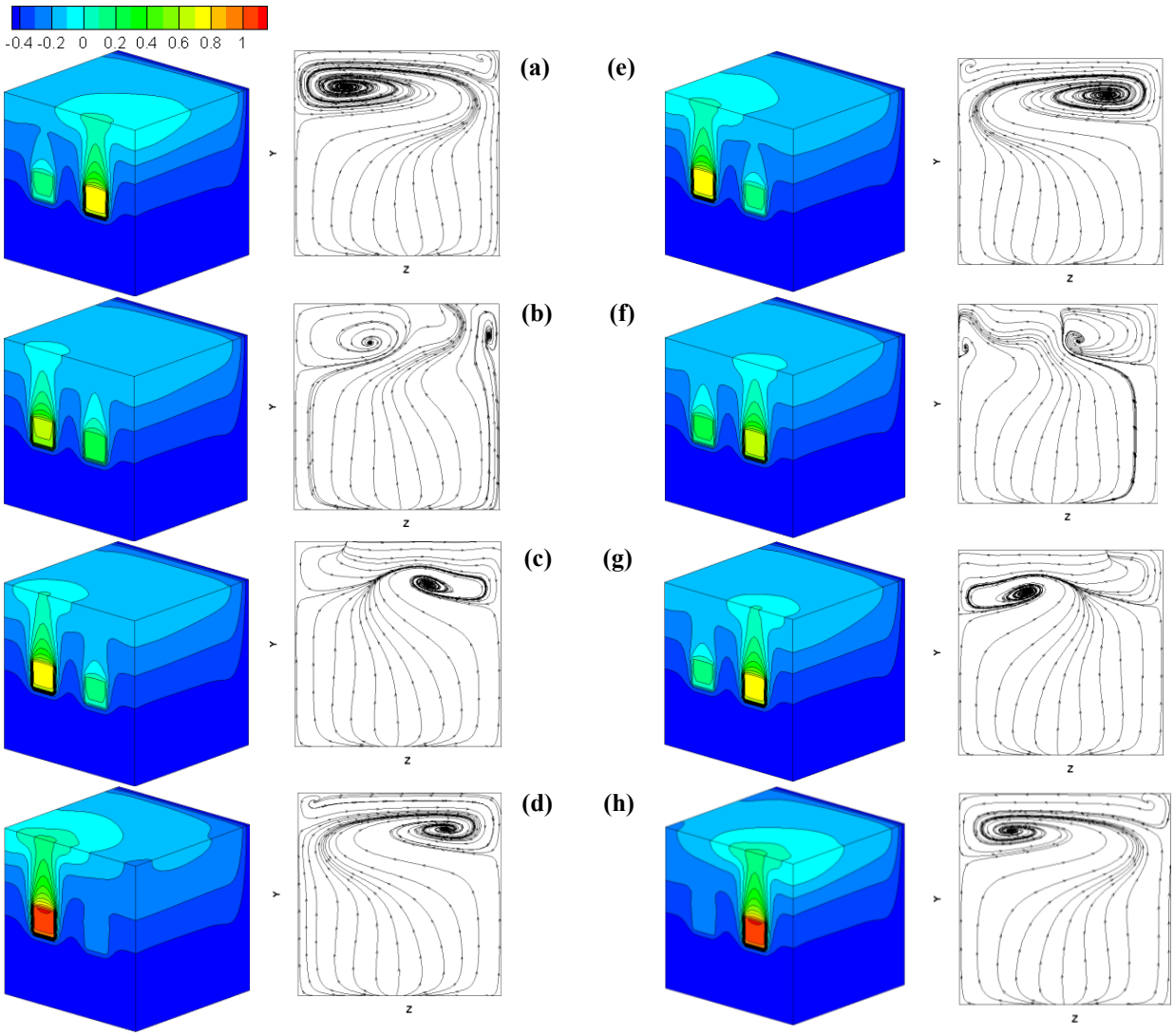

Figure 7. Isotherms and streamlines at plan X = 0.5 over one cycle for Ra = 10^6, a = 0.8 and τ_P = 0.2 in the case of two temperatures varying in opposition of phase.

In the case of the two temperatures varying in phase (figure 8a), $\overline{Nu_C}$ present peaks for the same value of the period of resonance (τ_P = 0.1), which is not affected by the increase of the amplitude. The improvement of heat transfer with respect to the steady state value ($\overline{Nu_C} = 2.0057$) is found to increase with a and reaches 2.06%, 6.7% and 13.8% respectively for a = 0.4, 0.8 and 1. Above this threshold, the increase of τ_P leads to a continuous weakening of the heat transfer until reaching minimum values which is higher than the steady value. It is to be mentioned that any increase of the amplitude contributes to the enhancement of the heat transfer through the cold wall of the cavity.

When the two temperatures are varied in opposition of phase (figure 8b), variations of $\overline{Nu_C}$ with τ_P are generally similar to those observed in the previous case. However, $\overline{Nu_C}$ present peaks for different values of the period which increases with the amplitude. Hence, the period of resonance was found to be equal to 0.1, 0.2 and 0.4 respectively for a equal to 0.4, 0.8 and 1. The enhancement of $\overline{Nu_C}$ with respect to the steady state value ($\overline{Nu_C} = 2.0057$) is then equal to 2.7%, 9.69% and 14.59% respectively when a is equal to 0.4, 0.8 and 1. Hence, this last mode present better heat transfer compared to the case of the two heating temperatures varying in phase.

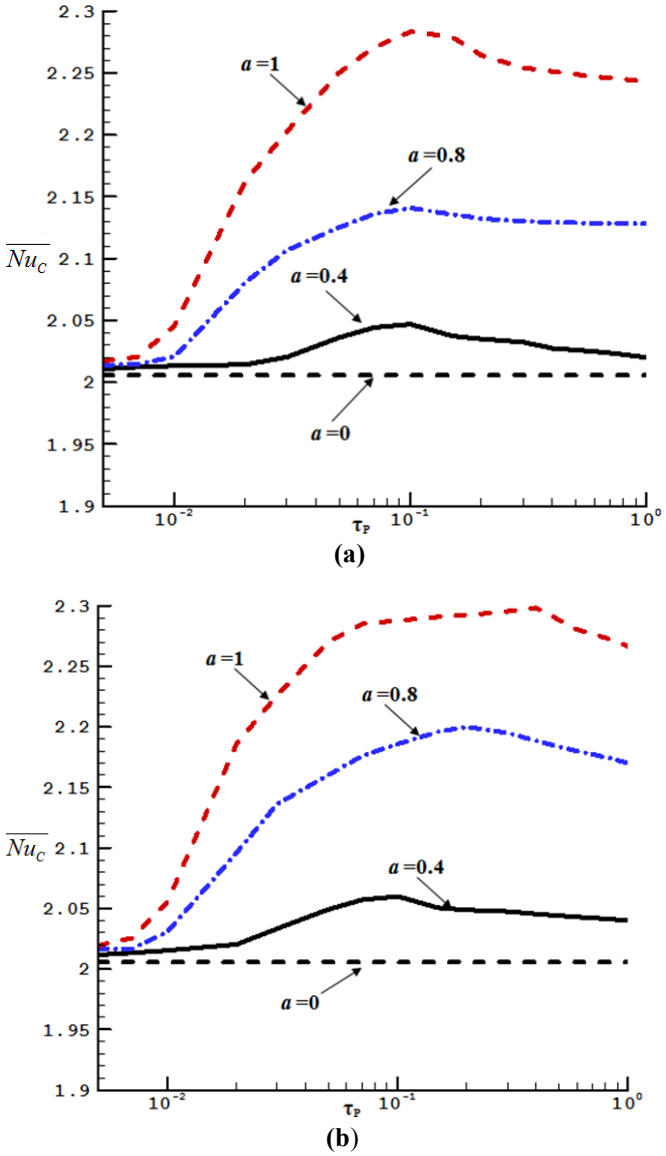

Fig. 8 Effect of τ_P for Ra =10^6 and various a: a) case of the two temperatures varying in phase b) case of the two temperatures varying in opposite phase.

4. Conclusion

The numerical study of natural convection in a cubical enclosure with two heating square sections submitted to periodic temperatures has identified the following conclusions:

- The average heat transfer through the cold wall of the cavity in the case of two variable temperatures is greater than its permanent value, if we except the case of short periods and small amplitudes;
- Varying the two temperatures in opposition of phase gives rise to a better heat transfer and an important fluid motion compared to the case of the two temperatures varying in phase.
- The resonant period, corresponding to the maximum mean heat transfer, depend on the imposed heating mode: In case the two temperatures varying in phase, it is close to the value 0.1 and independent of the excitation temperatures amplitudes, while it varies with the amplitude in the case of the two temperatures varying in opposition of phase.

Nomenclature

A = Dimensional amplitude of the heating temperatures
a = Dimensionless amplitude of the heating temperatures , Eq. (9)
D = Side of the square hot sector
g = Gravitational acceleration
L = cavity side
Nu = Average Nusselt number, Eq. (10)
Pr = Prandtl number, Eq. (7)
P = Non-dimensional pression
p = Pression N/m^2
Ra = Rayleigh number, Eq. (7)
T = Température
t_P = dimensional period
ΔT = Overall temperature diference, $(\overline{T_H} - T_C)$
u,v,w = dimensional velocities
U,V,W = dimensionless velocities, Eq. (6)
x, y, z = dimensional coordinates
X,Y,Z = dimensionless Cartesian coordinates, Eq. (6)

Greek symbols

α = thermal diffusivity
θ = non-dimensional temperature, Eq. (6)
β = volumetric thermal expansion coefficient
τ = non-dimensional time, Eq. (6)
τ_P = non-dimensional period, Eq. (9)
υ = kinematic viscosity
ρ = density
φ_P = dephasing, Eq. (8b)

Subscripts:

C = cold
H = hot
Nu = Nusselt number
H1 = heating section 1
H2 = heating section 2
r = Resonance

Superscripts

— = Time averaged quantity

References

[1] S. Ostrach, "Natural convection in enclosures", Int. J. Heat Transfer, Vol. 110, 1988, pp. 1175–1190.
[2] A. Bejan, and A. D. Kraus, Heat Transfer Handbook. Wiley, New York, 2003.
[3] R.J. Goldstein, et al., "A review of 2003 literature", Int. J. of Heat and Mass Transfer, vol. 49, 2006, pp 451-534.
[4] H. H. S. Chu, S. W. Churchill, and C.V.S. Patterson, "The effect of heater size, location, aspect ratio, and boundary conditions on two-dimensional, laminar, natural convection in rectangular channels", Int. J. Heat Transfer, vol. 98, 1976, pp. 195-201.
[5] B.L. Turner and R.D. Flack, "The experimental measurement of natural convective heat transfer in rectangular enclosures with concentrated energy sources", Int. J. Heat Transfer, vol. 102, 1980, pp. 237-241.
[6] N. Nithyadevi, P. Kandaswamy and J. Lee, "Natural convection in a rectangular cavity with partially active side walls", Int. J. of Heat Mass Transfer, vol. 50, 2007, pp. 4688–4697.
[7] D. Qi-Hong, "Fluid flow and heat transfer characteristics of natural convection in square cavities due to discrete source–sink pairs", Int. J. of Heat Mass Transfer, vol 51, 2008, pp. 5949–5957.
[8] T. Dias and L.F. Milanez, "Optimal location of heat sources on a vertical wall with natural convection through genetic algorithms", Int. J. Heat Mass Transfer, vol. 49, 2006, pp. 2090–2096.
[9] P. Vasseur and L. Robillard, "Natural Convection in a Rectangular Cavity With Wall Temperature Decreasing at a Uniform Rate", Waerme- Stoffuebertrag, vol. 16, 1982, pp. 199–207.
[10] J.I. Lage, A. Bejan, "The resonance of natural convection in an enclosure heated periodically from the side", Int J Heat Mass Transfer, vol. 36, 1993, pp. 2027–2038.
[11] B. Abourida, M. Hasnaoui and S. Douamna, "Convection Naturelle dans une Cavité Carrée avec des Parois Verticales Soumises à des Températures Périodiques", Rev. Gen.Therm, vol. 37, 1998, pp 788–800.
[12] B. Abourida, M. Hasnaoui and S. Douamna, "Transient natural convection in a square enclosure with horizontal walls submitted to periodic temperatures", Numerical Heat Transfer, PartA, vol. 36, 1999, pp. 737–750.
[13] I.E. Sarris, I. Lekakis, and N.S. Vlachos, "Natural convection in a 2D enclosure with sinusoidal upper wall temperature", Numer Heat Transfer, vol 36, 2002, pp. 513–520.
[14] C.Y. Soong, P.Y. Tzeng and C.D. Hsieh, "Numerical study of bottom-wall temperature modulation effects on thermal instability and oscillatory cellular convection in a rectangular enclosure", Int. J. of Heat and Mass Transfer, vol 44, 2001, pp. 3855-3868.
[15] N. Ben Cheikh, B. Ben Beya and T. Lili, "Aspect ratio effect on natural convection flow in a cavity submitted to a periodical temperature boundary", Int. J. Heat Transfer, vol. 129, 2007, pp 1060–1068.
[16] I. Sezai and A. Mohamad, "Natural convection from a discrete heat source on the bottom of a horizontal enclosure", Int. J. of Heat and Mass Transfer, vol. 43, 2000, pp 2257-2266.
[17] N. Ben-Cheikh, A. Campo, N. Ouertatani and T. Lili, "Three-dimensional study of heat and fluid flow of air and dielectric liquids filling containers partially heated from below and entirely cooled from above", Int. J. Heat Transfer, vol. 37,2010, pp 449–456.
[18] P.H. Oosthuizen and J. T. Paul, "Natural convection in a rectangular enclosure with two heated sections on the lower surface", Int. J. Heat and Fluid Flow, vol. 26, 2005, pp 587–596.
[19] R.L. Frederick and F. Quiroz, "On the transition from conduction to convection regime in a cubical enclosure with a partially heated wall", Int. J. Heat Transfer, vol. 44, 2001, pp 1699–1709.
[20] G. Wang, M. Zeng, Y.C. Ren, H. Ozoe and Q.W. Wang, "Transient heat flux measurement of natural convection in an inclined enclosure with time-periodically-varying wall temperature", Experimental Thermal and Fluid Science, vol. 35, 2011, pp 105–111.
[21] S.V. Patankar, "Numerical Heat Transfer and Fluid Flow". McGraw-Hill, New York, 1980.
[22] T. Fusegi, J.M. Hyun, K. Kuwahara and B. Farouk, "A numerical study of three-dimensional natural-convection in a differentially heated cubical enclosure", Int. J. Heat Mass Transfer, vol. 34, 1991, pp 1543-1557.

Lahoucine Belarche was born in Agadir, Morocco. He received a License degree from ENSET School, Mohamed 5 Souissi University Rabat, and a master degree from ENSA School, Ibn Zohr University Agadir in 2010. He is currently working toward the PhD degree in Computational fluid dynamics and thermal simulation engineering research at ENSA School, Ibn Zohr University Agadir, Morocco.

Btissam Abourida is currently a Professor (Professeur Habilité) at the Energy and environment engineering process department of National School of Applied sciences (ENSA), Ibn Zohr University, Agadir, Morocco, since 2008. She received her PhD degree in 1999 at cadi Ayyad University (Morocco), in Energy specialty. Her current research interests heat transfer phenomenon and renewable energy. She is responsible of energy and transfer phenomenon research team at ENSA.

Touria Mediouni is currently a Professor at the Energy and environment engineering process department of National School of Applied sciences (ENSA), Ibn Zohr University, Agadir, Morocco, since 1998. She received her PhD degree in 1994 at cadi Ayyad University (Morocco), in Energy specialty. Her current research interests evaporation and condensation, cooling machine, solar energy. She is director of the mechanics, energy and environment laboratory LMPEE.